S ORIGINAL ARTICLE

Shoulder & Elbow

Shoulder & Elbow
2019, Vol. 11(1S) 77–85
© The Author(s) 2018
Article reuse guidelines:
sagepub.com/journals-permissions
DOI: 10.1177/1758573218779078
journals.sagepub.com/home/sel
SAGE

Biomechanical testing of trans-humeral all-suture anchors for rotator cuff repair

Mikel Aramberri-Gutiérrez[1], Amaia Martínez-Menduiña[2], Simon Boyle[3] and Maria Valencia[4]

Abstract

Background: Rotator cuff tears are one of the most common causes of shoulder pain. All-suture anchors are increasingly being used in the arthroscopic repair of rotator cuff tears. The purpose of this experimental study is to evaluate the biomechanical properties of all-suture anchors at different insertion sites in the proximal humerus relevant to rotator cuff repairs and the remplissage procedure.

Methods: Sixteen cadaveric shoulders were used for the study. Four all-suture anchors were inserted in each proximal humerus at common anchor insertion sites on the rotator cuff footprint and a simulated Hill–Sachs defect. Cyclic loading and load-to-failure tests were undertaken. The number of cycles, load to failure and nature of failure were recorded.

Results: The all-suture anchors placed in the cuff footprint using a transosseous technique displayed superior biomechanical properties. Sutures sited in this way demonstrated a maximum tensile load to failure of 542 N as well as a highest mean load to failure and the maximum number of cycles before anchor failure. In descending order, all-suture anchors placed in the lateral footprint were significantly superior to those located in the medial row and in a simulated Hill–Sachs defect.

Discussion: Anchors placed in the rotator cuff footprint exceeded the physiological isometric abduction forces for the supraspinatus and infraspinatus. Data obtained from our study suggest that all-suture anchors are strong enough to be used for the repair of rotator cuff tears.

Keywords

rotator cuff repair, all-suture anchors, biomechanical testing

Date received: 11th April 2018; accepted: 3rd May 2018

Introduction

Rotator cuff tears (RCTs) are one of the most common causes of shoulder pain and dysfunction in adults, with an incidence of 87/100,000 persons-year.[2] The highest incidence of this pathology is seen in women between 55 and 59 years.[2–4] Furthermore, over 33% of all orthopaedic injuries involve rotator cuff pathology.[3]

For acute tears or where conservative management of chronic rotator cuff pathology fails, surgical treatment may be considered.[3,5] The all-arthroscopic rotator cuff repair is becoming the most commonly undertaken procedure for RCTs.[6] Different anchor designs and materials have been utilised for this procedure; however, the all-suture anchor is becoming an increasingly popular device. The principle of the all-suture anchor fixation relies on the increased diameter of the concertinaed anchor, once it has been deployed. Due to the small diameter of the suture anchor prior to deployment, a smaller drill hole can be made in the footprint of the greater tuberosity, therefore preserving a greater tendon-to-bone contact area, compared with traditional larger diameter anchors.[7] This is particularly important in cases of revision surgery where a

[1]Alai Sports Medicine Clinic, Madrid, Spain
[2]Hospital Universitario Ramon y Cajal, Madrid, Spain
[3]York Teaching Hospital, York, UK
[4]Fundacion Jimenez Diaz, Orthopaedics; Shoulder and Elbow Unit, Madrid, Spain

Corresponding author:
Mikel Aramberri-Gutiérrez, Alai Sports Medicine Clinic, Madrid, Spain
Email: aramberri@centroalai.es

significant part of the footprint available for tendon healing may be occupied by pre-existing traditional anchors.

The purpose of this study was to evaluate the resistance and maximum tensile load to failure of the all-suture anchor in order to determine the suitability of these anchors for RCT repair and remplissage procedures, as described by Purchase et al.[8]

Material and methods

Specimens

Sixteen fresh-frozen human shoulders were used in this study (15 male and one female). The average age of the specimens was 67.50 ± 4.69 years (range 55–74 years). As per similar peer reviewed biomechanical studies,[9,10] a power analysis was performed with PS Power and Sample Size Calculation Software (http://biostat.mc.vanderbilt.edu/PowerSampleSize). In order to detect a difference of 40 N at 2 mm of displacement with standard deviation (SD) = 19 N, $\alpha = 0.05$ and power of $(1-\beta) = 0.8$, our calculation determined that six specimens per type of anchor were required.[9,10]

The shoulder specimens were stored at −21°C in a freezer after which they were transferred to a refrigerator (4°C) for 24 h before dissection. Prior to dissection, CT scans of all shoulders were obtained to ensure there was no previous surgery or structural compromise to the humeral heads. All dissection and biomechanical measurements were performed at room temperature and the specimens were kept moist during the testing procedure using a 0.9% NaCl solution. Specimens were dissected to remove all soft tissues and the humerus was osteotomised through the humeral diaphysis at a distance of 12 cm distal to the greater tuberosity prior to biomechanical testing.[11–15] A Hill–Sachs defect[16–19] was created on each specimen using an oscillating saw. This allowed us to place anchors within a simulated defect for biomechanical testing of remplissage type fixation. The defect was measured from the infraspinatus tendon insertion (this was localised and marked in all the cadavers before dissection) as defined by Nozaki et al.[20] The dimensions for the defect were 2 cm from superior to inferior, 3 cm from medial to lateral and 0.5 cm in depth (Figure 1).

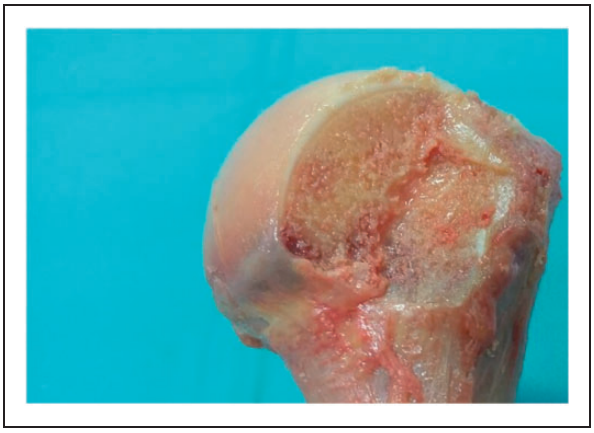

Figure 1. Figure shows the Hill–Sachs defect created on each shoulder for testing anchor (anchor number 4). The dimensions of the defect are 2 cm from superior to inferior, 3 cm from medial to lateral and 0.5 cm in depth, measured from the infraspinatus footprint.

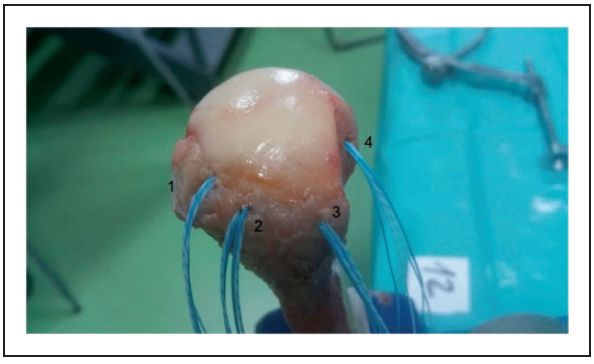

Figure 2. Anchor placement on the cuff rotator footprint. 1 – Medial row anchor, 2 – 14 mm lateral and slightly posterior to the first anchor (ATOR), 3 – lateral row anchor and 4 – anchor placed on the Hill–Sachs defect.

Anchor placement

Four 2.3 mm all-suture ICONIX® (Stryker Endoscopy, San Jose, USA) anchors were placed according to manufacturer's instructions in predetermined sites. The anchors were inserted by the senior author, an experienced shoulder arthroscopist, taking care to avoid trauma to the cortical bone of the greater tuberosity, using the anchor guide and avoiding footprint decortication. The anchors were placed as follows (Figure 2):

Position 1) 14 mm posterior to the bicipital groove and immediately adjacent to the cartilage of the humeral head (medial row anchor)

Position 2) 14 mm lateral and slightly posterior to the first anchor using a complete humeral transosseous tunnel to allow the anchor to be deployed medially at the humeral calcar (ATOR technique)[7]

Position 3) 14 mm posterior to the second anchor (lateral row)

Position 4) in the created Hill–Sachs defect 2 mm lateral to the cartilage and centred in the defect (from superior to inferior) of the posterior humeral head. The angle of insertion of the implants placed in positions 1, 2 and 3 was 45° and for position number 4 this was 90°.[21] Position 4 would replicate the anchor position

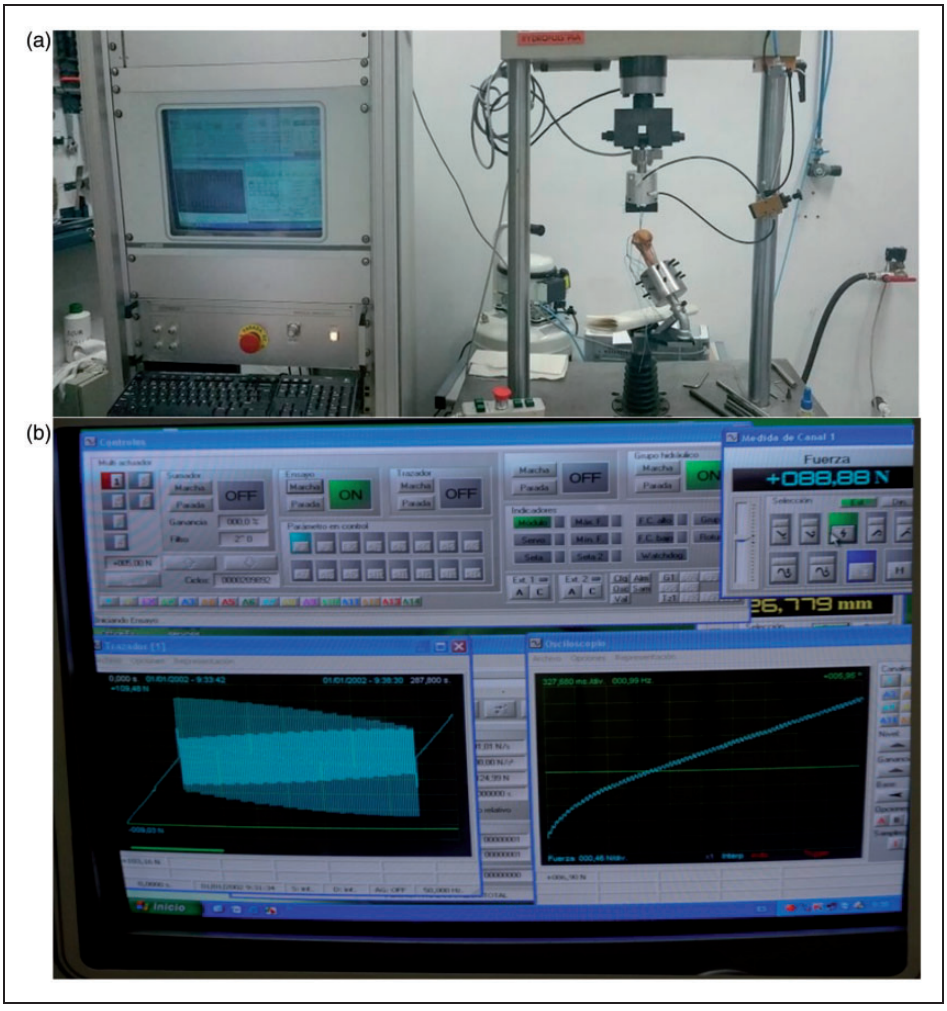

Figure 3. (a) Figure shows shoulders placed on the servo-hydraulic testing machine for cyclic loading and pull-out testing (model HYDROPULS PSA, SCHENCK, Germany) and (b) computer recording of the graphic representation of the relationship between suture anchor displacement and tension during the biomechanical testing. PCD2K software system (Servosis Ltd, Madrid, Spain).

for the remplissage technique as described by Purchase et al.[8]

Biomechanical testing

Cyclical load testing was used in the biomechanical evaluation in order to simulate the loads experienced during the postoperative period of a rotator cuff repair.[12,13] A servo-hydraulic testing machine (model HYDROPULS PSA, SCHENCK, Germany) was utilised containing a 2 kN HBM load cell (range 10 N to 2 kN) and an uncertainty of measurement of 0.2%. Data acquisition and recording was performed using the PCD2K software system (Servosis Ltd, Madrid, Spain) (Figure 3(a)). The software allowed the display of a continuous graphic representation of the relationship between suture anchor displacement and tension throughout testing (Figure 3(b)).

To ensure secure specimen fixation for testing, it was necessary for the distal end of each specimen to be coated with bone cement (Cementex Rx, Tecres) and fixed with a double row configuration of blunt screws. In total, eight screws were required to secure the distal humerus to the base of the testing apparatus which was set at an angle of 135°. This orientation was chosen to replicate the physiological direction of pull of the supraspinatus tendon within our experimental set-up[10,14,22,23] (Figure 4). This configuration also permitted the precise adjustment of the direction of pull of the sutures. The sutures were secured at a distance of 5 cm from the anchor.[14,24]

The phases and the number of load cycles were selected to emulate Barber's studies.[11,12,25] Load and displacement values were recorded throughout the testing process. The initial anchor displacement was determined once the test set-up was stabilised

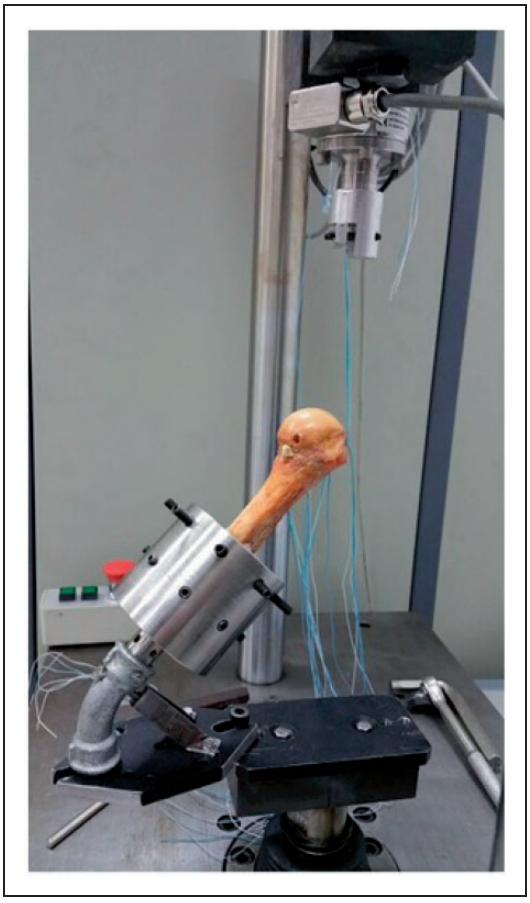

Figure 4. Placement of anatomical pieces for biomechanical testing. Humeral head and 12 cm of humeral shaft with a pull-out angle of 135° to replicate physiological direction of pull of the supraspinatus tendon.

after 10 cycles of pre-loading. Cyclical load testing involved the application of a preload of 10 N with a crosshead extension rate of 1 N/s. The loading history of each sample was divided into three phases. During all phases, the tensile load was applied over 100 cycles with a frequency of 0.5 Hz. The first phase involved a sequential increase in tension between 10 and 100 N, the second phase between 100 and 150 N and the final phase between 150 and 200 N.

The number of cycles completed until anchor failure and the mode of failure (suture anchor rupture, migration or bone fracture) were recorded for the study.

Finally, a destructive test was conducted at a rate 20 mm/min until failure of the anchor fixation construct.

Bone mineral density (BMD)

The BMD was measured for all shoulder specimens in two distinct regions: the greater tuberosity and the calcar anchor deployment site. The scanning equipment was calibrated to perform a shoulder scan, Hologic Osteoporosis Assessment, software system apex 3.0; Explorer model series number 91708, system Id. A (revision date 12 November 2013) (Figure 5).

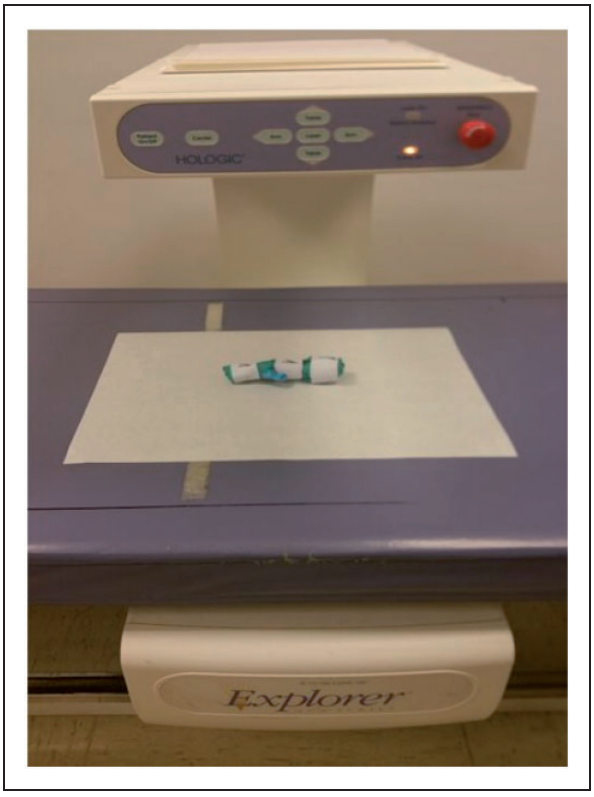

Figure 5. BMD testing of cadaver shoulders (Hologic Osteoporosis Assessment, software system apex 3.0; Explorer model series number 91708, system Id. A, last revision date 12 November 2013).

For each location (calcar and greater tuberosity) three data values were measured: area (cm^2), mineral bone quantity (CMO) (g) and BMD (g/cm^2). In order to evaluate bone quality, BMD data for each specimen were used for comparison.

Statistical analysis

Descriptive analysis was performed for all variables (frequency for categorical variables and mean and SD for continuous variables).

In order to satisfy the study objectives, bivariate tests were employed. According to non-parametric Kolmogorov–Smirnov test, all relevant variables are normally distributed. One-way analysis of variance with HSD Turkey post hoc tests was applied to study the possible significant differences between the failure loads and displacement for the four fixation sites. Linear Pearson correlation was performed in order to test any potential significant relationship between the BMD and failure loads of the four fixation sites. The significance level for all analyses was 5%.

Any p-value less than this were considered to be a statistically significant relationship ($P < .05$).

The statistical analysis was performed with IBM SPSS Statistics 22.

Results

During the testing process, three anchors test set-ups were abandoned due to technical difficulties with the testing machine. One of these failed tests occurred with the anchor placed in position 2 (specimen 1) and the other two technically failed tests occurred with anchors placed in position 3 (specimen 1 and 7). This reduced the sample size of the anchors tested from 64 to 61.

The cyclic loading and force-to-failure values were recorded for the four described anchor positions within the humeral head. The maximum tensile load supported by any anchor was 541.99 N when a destructive test was applied. The load to failure was highest for the anchor placed in position 2, i.e. the transosseous anchor (ATOR). For this anchor position, the mean failure load was 315.61 ± 126.27 N (Table 1). In order to determine significant differences among results, a one-way ANOVA was performed. The overall results show that there were significant differences ($F = 23.24$, $P < 0.01$) between anchor sites. This analysis revealed that under biomechanical testing (cyclic loading and ultimate load to failure) for anchors placed in position 2 (complete transosseous – ATOR) were significantly greater than those located in position 1 (medial row, 150.64 ± 59.04, $P < .001$), position 3 (lateral row, 223.17 ± 87.97, $P = .035$) and position 4 (Hill–Sachs defect, 118.43 ± 50.34, $P < .001$) (Table 1).

In addition, 14 of the 15 anchors placed in position 2 survived the complete cyclical load testing protocol after which ultimate load to failure was performed. For anchors placed in position 1, 3 and 4 only 2, 7 and 0 anchors, respectively, survived the cyclical loading regime and went on to undergo failure testing.

A one-way ANOVA analysis revealed significant differences in the mean values of failure strength of the anchors in the different positions ($F = 8.28$, $P < .001$). In descending order of mean failure resistance: position 2 > position 3 > position 1 > position 4.

When reviewing the number of cycles supported by each anchor, the results indicated that the anchor in position 2 (ATOR) permitted the highest average number of cycles to failure (267.14 ± 70.08) followed by the anchor located in position 3 (lateral row, 214.92 ± 106.17) (Table 2). The average number of cycles in position 2 was significantly higher than the average number in position 1 (medial row, 173.33 ± 94.02, $P = .041$) and 4 (Hill–Sachs defect, 93.20 ± 68.98, $P = .000$). There was also significant difference between position 3 and 4 ($P = .009$).

The amount of anchor displacement was recorded during cyclic loading. The mean cyclic displacement (±SD) for each anchor is shown in Table 3. The results of the one-way ANOVA analysis revealed that there were significant differences in the average value of displacement during the first and second phases at 99% (first phase: $F = 11.19$, $P < .001$; second phase: $F = 5.45$, $P = .004$), and at 95% during the third phase ($F = 5.11$, $P = .016$). During the first two phases, the anchor in position 4 (Hill–Sachs, $2.21 \pm .63$ and $2.05 \pm .47$)

Table 2. Number of cycles/shoulder. The results indicated that the anchor in position 2 permitted the highest average number of cycles to failure.

	N	Mean ± SD	Minimum	Maximum
Anchor 1	12	173.33 ± 94.02	3	300
Anchor 2	14	267.14 ± 70.08	48	300
Anchor 3	13	214.92 ± 106.17	1	300
Anchor 4	10	93.20 ± 68.98	1	203

Table 1. Descriptive statistics. The load to failure was highest for the anchor placed in position 2. These results were significantly superior to those located in positions 1, 3 and 4.

	N	Minimum	Maximum	Mean	Stand. dev
Anchor 1	16	40.79	257.00	150.64	59.04
Anchor 2	15	100.00	541.99	315.61	126.27
Anchor 3	14	100.00	394.73	223.17	87.97
Anchor 4	16	9.06	200.00	118.43	50.34
N Valid	14				

Table 3. Displacement during cyclic loadings.

	10–100 N		100–150 N		150–200 N	
Anchor	N	Mean ± SD (mm)	N	Mean ± SD (mm)	N	Mean ± SD (mm)
Anchor 1	12	1.32 ± .66	8	1.11 ± .46	3	.79 ± .25
Anchor 2	15	1.67 ± .71	13	1.68 ± .87	12	1.50 ± .81
Anchor 3	13	.89 ± .31	11	.80 ± .53	10	.69 ± .31
Anchor 4	13	2.21 ± .63	4	2.05 ± .47	0	–
	F = 11.19 (P < .001)		F = 5.45 (P = .004)		F = 5.11 (P = .016)	

showed a significant higher displacement than anchors 3 (lateral row) and 1 (medial row). This is most likely due to the absence of cortical fixation. Conversely, anchor fixation at the medial row (anchor 1) and lateral row (anchor 3) showed the lowest mean value of displacement. In these sites, the cortical bone was preserved.

During the third phase of testing (150 to 200 N), the anchor in position 2 (ATOR) demonstrated the highest mean displacement (1.50 ± .81). This is likely due to progressive loss of cortical fixation at the medial calcar.

Failure modes were registered for each anchor. All anchors placed in position 1 (medial row), 3 (lateral row) and 4 (Hill–Sachs) failed due to complete anchor pull out. Anchors placed in position 2 (ATOR) failed due to migration of the anchor from the calcar region to the inside of the humeral head (resulting in loss of tension in the sutures). Anchor position 2 was most resistant to failure (only 20% of failures) followed by anchor 3 (28.57%).

Further tests were performed with qualitative variables to analyse the relationships between anchor pull-out resistance and age. No significant findings were obtained for the age-resistance correlation.

A linear correlation analysis was performed in order to assess the possible association between maximum failure load and BMD of the patient. These results indicated that there was a positive association between BMD at humeral calcar and resistance to failure with anchor in position 1 (r = .38, P = .151), anchor in position 2 (r = .17, P = .538), anchor in position 3 (r = .29, P = .308) and anchor in position 4 (r = .05, P = .857). In shoulders with high BMD, a higher pull-out resistance of the anchor was seen. In the case of bone densitometry at the greater tuberosity, a negative relationship was found in relation to anchor pull-out resistance. This can be seen in position 2 (r = −.38, P = .166), position 3 (r = −.15, P = .612) and the anchor in position 4 (r = −.08, P = .758). These results were not found to be statistically significant.

Discussion

Despite improvements in arthroscopic techniques, successful rotator cuff repair surgery presents challenges, particularly given the reported high re-tear rate. Although biological factors are often implicated in failures of rotator cuff healing, it is hoped that new anchor technology and materials may help improve tendon healing.[9,13,14] The use of the remplissage technique has also been increasingly been used as an adjunct in glenohumeral instability surgery. This requires the insertion of anchors into the humeral head to secure the rotator cuff into a bony defect and necessitates cuff healing at this defect site.[16–18]

Modern all-suture anchors have been designed to reduce the area that a traditional anchor occupies on the greater tuberosity cuff footprint whilst maintaining optimal pull-out strength. This new design preserves more humeral bone surface area at the footprint as compared to classic anchors; therefore, they potentially increase the area for tendon-to-bone contact. This could be particularly important for revision rotator cuff repairs. Currently, it is unclear as to the optimal site of insertion of the all-suture anchor in the footprint area for rotator cuff repair surgery.

The purpose of this study was to evaluate the resistance and maximum tensile load to failure of an all-suture anchor placed in the humeral head. This knowledge would assist in determining the suitability of these anchors for use in rotator cuff repairs and remplissage procedures and also to determine the optimal tuberosity insertion site with regards to anchor pull out. Dynamic cyclical load testing at a physiologic pull-out angle and tension was undertaken to replicate the rotator cuff biomechanics in the postoperative period.[9,11,14,15,17,22,24]

The isometric tensile forces for the rotator cuff tendons have been determined in a cadaveric model as 117 N for the supraspinatus tendon and 205 N for the infraspinatus tendon in maximum effort.[26] Our study sought

to determine whether the all-suture anchor pull-out resistance is sufficient to support physiological rotator cuff tendon forces. Previous pull-out studies have shown similar results with all-suture anchors 173–333[15] and 100–225 N[24] and with classic screw in anchors 75–225[14] and 90–200 N.[24] Our study demonstrated a maximum tensile load to failure of 541.9 N. This value was observed for the anchor placed in position 2 (ATOR) where the all-suture anchor was passed from the greater tuberosity to the humeral calcar to take advantage of the cortical bone found in this region. The mean failure load at this site was 315 N (188.7–541.9). These data are superior to other results in the literature.[14,15,24] The reason for the superiority of anchor placed in position 2 is the transosseous concept using an all-suture anchor allowing a complete transosseous configuration performed all arthroscopically.[7] The basis of this stronger fixation relies on the increase in diameter of the anchor (4 mm once deployed versus drill hole size 2.3 mm). The anchor is then directly opposed to the thicker cortical bone of medial humeral calcar. This technique may be particularly useful in revision cases, where there is soft tuberosity bone or when facing failed fixation using any anchor type at the greater tuberosity.

The pull-out force results revealed the maximum tensile load to failure supported by an anchor; however, we also employed dynamic cyclical load testing to best replicate physiological rotator cuff use. All the anchors placed in position 2 (ATOR) and seven of the anchors placed in position 3 (lateral row) continued to support a 200 N load after 300 cycles. These results exceed those reported in biomechanical studies of physiological simulations of supraspinatus and infraspinatus isometric forces.[26]

Data obtained from this study suggest that anchors placed in positions 1, 2 and 3 are strong enough to be used in the repair of RCTs.

Anchors placed in the posterosuperior position (Hill–Sachs lesion) in order to simulate a remplissage technique (anchor 4) demonstrated a lower resistance to pull out than all other positions (mean force 118.43 N). The predicted maximum isometric force for infraspinatus in cadaveric studies is 205 N. This lower pull out may be secondary to the artificial fashion in which the Hill–Sachs lesion was created whereby a segment of corticocancellous bone was removed. This is different to the impaction mechanism that occurs in vivo during a dislocation. Due to these biomechanically inferior results, the use of all-suture anchors for remplissage procedures should be further evaluated and cannot be recommended based on this current biomechanical testing.

Although some studies have found a relationship between lower pull-out resistance and osteoporotic bone,[15] we found no clear relationship between osteoporosis and all-suture anchor failure. This may be due to the small sample size in our study. Further studies are needed to determine the association between all-suture anchor failure and osteoporosis. No statistically significant association was found between age and anchor pull-out resistance.

Barber et al.[25] tested all-suture anchors in fresh porcine cortical bone and polyurethane foam blocks through cyclic loading, followed by a destructive test. Their results are not directly comparable to our study for several reasons. In our study, we used fresh human proximal humeral specimens with an average age of 67.50 ± 4.69 years (range 55–74 years). Our study also differed from that of Barber et al., as our construct tested the anchors along the axis of contraction of the supraspinatus, better replicating physiological forces. Our cyclic loading phases reached 200 N as compared to the 100 N reached by Barber et al. These differing conditions may have a relationship with the failure mode and values.

Regarding the failure mode, the anchors placed in position 1, 3 and 4 failed due to avulsion pull out. The anchors placed in position 2 (ATOR) failed due to migration of the deployed anchor inside the humeral head resulting in detensioning of the sutures. None of the anchors failed due to suture breakage as compared to findings in the literature.[10–14,25]

When we evaluated anchor displacement there was a significantly lower mean displacement seen for the medial and lateral row anchors during the first and second phase of cyclical testing. We believe this occurs due to the good subcortical fixation of the anchors once they have been deployed. The anchor placed in the simulated Hill–Sachs defect showed significantly higher displacement. We believe this is secondary to the absence of subcortical fixation. To our knowledge, this is the first study showing a strong pull-out strength at both medial and lateral rows with a very low displacement rate at these locations using all-suture anchors.

This study has several limitations. First, all the soft tissues on the specimens were dissected and removed including the native rotator cuff, rather than recreating a tear in the rotator cuff and simulating a surgical repair. However, the purpose of this study was to determine all-suture anchors resistance in different footprint areas regardless of the rotator cuff injury, quality or type of suture repair. A further limitation would be the lack of a control group using either traditional anchors or different commercially available all-suture anchors. Additionally, no greater tuberosity footprint decortication was undertaken before placing the anchors, whereas light decortication may be performed by some surgeons in rotator cuff repair patients.

A final limitation of the study is the simulated Hill–Sachs lesion we created as described by Sekiya et al.[19] and Degen et al.[27] Our defect represents an osteotomy

rather than a true impaction defect. This may well affect the local bone density and pull-out strength results.

Conclusion

We have demonstrated the biomechanical properties of an all-suture anchor model for use in rotator cuff repairs and remplissage procedures. The ultimate load to failure for anchors placed in the medial and lateral row of the cuff footprint exceeded the physiological isometric abduction forces for the supraspinatus and infraspinatus (117 and 205 N). Data obtained within our study support the use of an all-suture anchor for performing double row rotator cuff repairs. Inferior results were seen when the all-suture anchor was used in a simulated Hill–Sachs defect.

Acknowledgements

Special thanks to the Engineers of UNED University, directed by Maite Carrascal, PhD, as well as Nuclear Medicine, Radiology and Orthopedic Surgery Departments and specially to our interns Carolina Hernández-Galera, Roque Pérez-Expósito, Rosa Vega-Rodríguez and Alejandro Lorente-Gómez who helped us in the dissection of all the shoulders. Also, thanks to María Fuentes-Blasco for her help in the statistical analysis.

Declaration of Conflicting Interests

The author(s) declared the following potential conflicts of interest with respect to the research, authorship, and/or publication of this article: Stryker paid 14,000 euros for the cadaveric shoulders to Scientific Anatomy, transport according to the local laws and incineration; and 6500 euros for the biomechanical testing to the engineering department of UNED university. Stryker also provided the Iconix anchors for performing the biomechanical testing.

Funding

The author(s) received no financial support for the research, authorship, and/or publication of this article.

Ethical Review and Patient Consent

This biomechanical study was approved by UNED University Ethics Committee.

References

1. Nagra NS, Zargar N, Smith RD, et al. Mechanical properties of all-suture anchors for rotator cuff repair. *Bone Joint Res* 2017; 6: 82–89.
2. White JJ, Titchener AG, Fakis A, et al. An epidemiological study of rotator cuff pathology using the Health Improvement Network database. *Bone Joint J* 2014; 96-B: 350–353.
3. Lee TQ. Current biomechanical concepts for rotator cuff repair. *Clinic Orthop Surg* 2013; 5: 89–97.
4. Jain NB, Higgins LD, Losina E, et al. Epidemiology of musculoskeletal upper extremity ambulatory surgery in the United States. *BMC Musculoskelet Disord* 2014; 15: 4.
5. Clement ND, Nie YX and McBirnie JM. Management of degenerative rotator cuff tears: a review and treatment strategy. *Sports Med Arthrosc Rehabil Ther Technol* 2012; 4: 48.
6. Pham TT, Bayle Iniguez X, Mansat P, et al. Postoperative pain after arthroscopic versus open rotator cuff repair. A prospective study. *Orthop Traumatol Surg Res* 2016; 102: 13–17.
7. Aramberri-Gutierrez M, Martinez-Menduina A, Valencia-Mora M, et al. All-suture transosseous repair for rotator cuff tear fixation using medial calcar fixation. *Arthrosc Tech* 2015; 4: e169–e173.
8. Purchase RJ, Wolf EM, Hobgood ER, et al. Hill-sachs "remplissage": an arthroscopic solution for the engaging Hill–Sachs lesion. *Arthroscopy* 2008; 24: 723–726.
9. Mazzocca AD, Chowaniec D, Cote MP, et al. Biomechanical evaluation of classic solid and novel all-soft suture anchors for glenoid labral repair. *Arthroscopy* 2012; 28: 642–648.
10. Goschka AM, Hafer JS, Reynolds KA, et al. Biomechanical comparison of traditional anchors to all-suture anchors in a double-row rotator cuff repair cadaver model. *Clin Biomech* 2015; 30: 808–813.
11. Barber FA and Herbert MA. Cyclic loading biomechanical analysis of the pullout strengths of rotator cuff and glenoid anchors: 2013 update. *Arthroscopy* 2013; 29: 832–844.
12. Barber FA, Herbert MA, Hapa O, et al. Biomechanical analysis of pullout strengths of rotator cuff and glenoid anchors: 2011 update. *Arthroscopy* 2011; 27: 895–905.
13. Goradia VK, Mullen DJ, Boucher HR, et al. Cyclic loading of rotator cuff repairs: a comparison of bioabsorbable tacks with metal suture anchors and transosseous sutures. *Arthroscopy* 2001; 17: 360–364.
14. Schneeberger AG, von Roll A, Kalberer F, et al. Mechanical strength of arthroscopic rotator cuff repair techniques: an in vitro study. *JBJS* 2002; 84-A: 2152–2160.
15. Tingart MJ, Apreleva M, Zurakowski D, et al. Pullout strength of suture anchors used in rotator cuff repair. *JBJS* 2003; 85-A: 2190–2198.
16. Buza JA 3rd, Iyengar JJ, Anakwenze OA, et al. Arthroscopic Hill-Sachs remplissage: a systematic review. *JBJS* 2014; 96: 549–555.
17. Elkinson I, Giles JW, Boons HW, et al. The shoulder remplissage procedure for Hill-Sachs defects: does technique matter? *J Shoulder Elbow Surg* 2013; 22: 835–841.
18. Tan BH and Kumar VP. The Arthroscopic Hill-Sachs remplissage: a technique using a PASTA repair kit. *Arthrosc Tech* 2016; 5: e573–e578.
19. Sekiya JK, Wickwire AC, Stehle JH, et al. Hill-Sachs defects and repair using osteoarticular allograft transplantation: biomechanical analysis using a joint compression model. *Am J Sports Med* 2009; 37: 2459–2466.
20. Nozaki T, Nimura A, Fujishiro H, et al. The anatomic relationship between the morphology of the greater

tubercle of the humerus and the insertion of the infraspinatus tendon. *J Shoulder Elbow Surg* 2015; 24: 555–560.
21. Green RN, Donaldson OW, Dafydd M, et al. Biomechanical study: determining the optimum insertion angle for screw-in suture anchors – is deadman's angle correct? *Arthroscopy* 2014; 30: 1535–1539.
22. Burkhart SS, Adams CR, Burkhart SS, et al. A biomechanical comparison of 2 techniques of footprint reconstruction for rotator cuff repair: the SwiveLock-FiberChain construct versus standard double-row repair. *Arthroscopy* 2009; 25: 274–281.
23. Burkhart SS, Diaz Pagan JL, Wirth MA, et al. Cyclic loading of anchor-based rotator cuff repairs: confirmation of the tension overload phenomenon and comparison of suture anchor fixation with transosseous fixation. *Arthroscopy* 1997; 13: 720–724.
24. Pietschmann MF, Froehlich V, Ficklscherer A, et al. Biomechanical testing of a new knotless suture anchor compared with established anchors for rotator cuff repair. *J Shoulder Elbow Surg* 2008; 17: 642–646.
25. Barber FA and Herbert MA. All-suture anchors: biomechanical analysis of pullout strength, displacement, and failure mode. *Arthroscopy* 2017; 33: 1113–1121.
26. Escamilla RF, Yamashiro K, Paulos L, et al. Shoulder muscle activity and function in common shoulder rehabilitation exercises. *Sports Med* 2009; 39: 663–685.
27. Degen RM, Giles JW, Johnson JA, et al. Remplissage versus latarjet for engaging Hill-Sachs defects without substantial glenoid bone loss: a biomechanical comparison. *Clin Orthop Rel Res* 2014; 472: 2363–2371.